Method Based on Triangulation for Sensor Deployment on 3D Surfaces

Renan Nespolo*, Leandro Alves Neves*, Guilherme Roberto*, Matheus Ribeiro*,
Marcelo Zanchetta do Nascimento† and Adriano Cansian*
*Department of Computer Science and Statistics (DCCE),
São Paulo State University (UNESP), São José do Rio Preto, Brazil
Email:renan.nespolo@sjrp.unesp.br
†FACOM, Federal University of Uberlândia, Uberlândia, Brazil

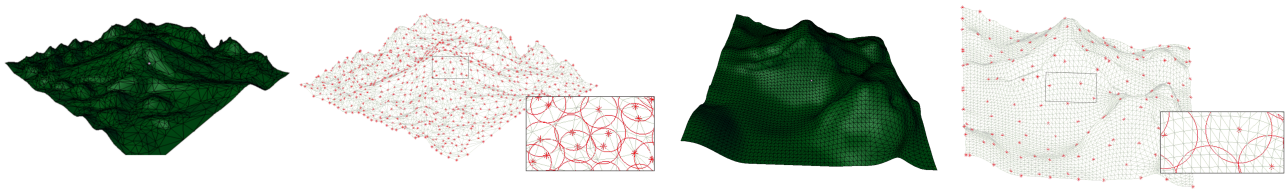

Fig. 1. Teasing result of our method: from this data input (left), the relevant feature are extracted using our technique (middle), producing effective result (right).

***Abstract*—In this work a new method is proposed to obtain the deployment of sensor nodes with a maximum coverage area using a minimum number of sensor nodes in three-dimensional surfaces. The deployment is performed using the dual Delaunay triangulation/Voronoi Diagram. The position selection process considered the vertices as candidate positions and the sensing radius. The positions were selected based on the maximum area coverage and the existence of communication among them. The communication was defined as omnidirectional. To ensure the coverage area, the problem of sensing superposition was considered. The verification of the communication is accomplished by the minimum spanning tree algorithm. To certify the versatility of the proposed method, we show the deployment in distinct surface areas commonly monitored by Wireless Sensor Networks. The results were significant, with coverage area between 84% and 95% for distinct types of reliefs.**

***Keywords*-Wireless Sensor Network; Sensor nodes; Deployment; Simulation;**

I. Introduction

Wireless sensor networks (WSN) consist in sensor nodes deployed on a surface. The goal of a WSN is to monitor events in the area of interest, such as natural or artificial origins. The sensor nodes are composed by memory, communication device, processor, sensing device, and battery. Each node that composes a WSN can be equipped with a variety of sensors, such as acoustic, seismic, infrared, camera, heat, temperature or pressure [1]. After the capturing and processing of the event, the sensor node can send the collected data by broadcast on the WSN [2].

The deployment of a WSN is highly dependent on the position of the sensor nodes in the area of interest. The challenge of the proposed method is the problem of minimum set coverage (MSC): obtaining the maximum coverage area using the minimum set of sensor nodes. Commonly, the best solutions are obtained by computer simulations [3], [4], [5], [6], [7], [8], [9], [10], [11], [12], [13]. When this strategy is explored, another challenge is the problem of the deployment in Three-dimensional surfaces: considering surfaces flattening may provide deployments of sensor nodes that do not properly solve the problem of MSC [3], [5], [6], [14].

In literature, the proposed methods considering three-dimensional solutions showed relevant results for specific reliefs [4], [7], indicating that it is possible to propose a flexible method to solve the problem of minimum set coverage on distinct three-dimensional surfaces.

In this work a new method is described to indicate candidate positions of sensor nodes to deploy them on three dimensional surfaces. The method was based on Delaunay triangulation, wherein each vertex is considered as a candidate position for the deployment of a sensor node. The criterion for selection of candidate positions was based on the intersection of sensing radii. The performance of the method was defined considering the coverage area and the existence of communication among selected positions by the minimum spanning tree algorithm. The results are promising, with higher coverage rates than showed in other methods available in literature. The main contributions are: 1. Deployment of sensor nodes for distinct three-dimensional surfaces commonly found in nature and used in WSN researches; 2. Proposal of a solution to the problem of minimum set coverage, providing relevant coverage rates; 3. Treatment of sensing superpositions and limits of coverage for three-dimensional surfaces.

A. Related work

Studies about sensor deployment were presented with highlights results, such as industrial monitoring [15], environmental [16], [17], [18], [19], air quality [20] and structural bridges [21]. However, few works are directed to realistic three-dimensional solutions. These results are based on evolutionary methods, Delaunay and Voronoi. The solutions of evolutionary methods provide interesting rates of coverage areas [5], [10], [11], [12], considering the radius of communication range [5], [10], [11] or sensing range [4], [7], [8], [12]. However, the complexity and performance are features that limit the processing of deployments in real time. Moreover, solutions based on Delaunay triangulation (DT) [22] and Voronoi diagram (VD) [23] provided results with a more uniformly deployment [3], [6]. But neither of mentioned works used the Delaunay triangulation vertices as candidate positions. Furthermore, these optimization techniques assist the initial distribution in real time with the sensor nodes' removals or movements. This feature allows the reduction of the number of sensor nodes deployed, without damaging the coverage rates and connectivity of the sensor nodes [5], [10], [11], [10].

In this context, the strategies for sensor deployment in three-dimensional surfaces were shown in [4], [7]. The results presented by [4] provided 46% of coverage area rate, using 2800 nodes for a three-dimensional rough terrain. The results presented in [7] provided 400 sensor nodes and obtained about 98% of coverage rate for an irregular surface. These works focused on defining the best deployment using approaches such as grid or randomness [4], [7]. The proposed method considered the Delaunay triangulation strategy, a different one from those indicated in these two works, making simulations for distinct three-dimensional surfaces.

B. Technique overview

The proposed method was structured in steps. At first, it is necessary to provide the three-dimensional surface which will be used to calculate the candidate positions of sensor nodes. In this work, the versatility of the method is shown as distributions of distinct surface areas commonly explored for WSN monitoring. The types of relief considered are: landing, hilly and surfaces used by [4] and [7]. The second step is to calculate the candidate positions using the Delaunay triangulation (DT). In the proposed method, each vertex of the triangulation was understood as a candidate position for a sensor node. This strategy was applied to provide a uniform deployment of sensor nodes. In the third step the candidate positions are selected considering the reference of sensing radius in meters and informed by the user. The positions were selected based on the maximum area coverage and the existence of communication among them. The communication was defined as omnidirectional (circumference) and represented by a radius. The fourth step allows to handle the problem of sensing superposition, to ensure actual coverage rates. The fifth step is to verify whether the candidate positions generate a connected set and full communication of WSN: the strategy adopted was to combine the minimum spanning tree algorithm and sensing radius. A flowchart of the proposed solution in this work is shown in Fig. 2.

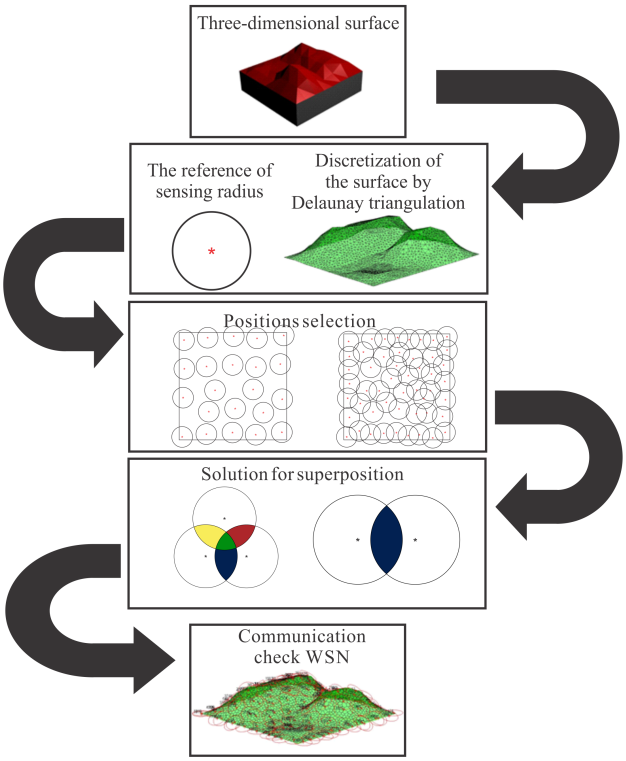

Fig. 2. Overview of the proposed method in steps for selection of candidate positions

II. Technical Background

The proposed method was based on Delaunay triangulation, which can be exposed by two definitions.

Definition 1. *A simplex K is a sorted list of vertices $\{P_i\}$ with $1 \leq i \leq d+1$, where d is a dimension of Euclidean space given by E. The determinant of order $d+1$ is called $det(K)$ and is given by:*

$$det(K) = \begin{vmatrix} 1 & \cdots & \cdots & \cdots & 1 \\ P_1^1 & \cdots & \cdots & \cdots & P_{d+1}^1 \\ P_1^2 & \cdots & \cdots & \cdots & P_{d+1}^2 \\ \vdots & \vdots & \vdots & \vdots & \vdots \\ P_1^d & \cdots & \cdots & \cdots & P_{d+1}^d \end{vmatrix}$$

where P_i^j is a coordinate j of point P_i for $1 \leq i \leq d+1$ and $1 \leq j \leq d$. By definition, if $det(K) > 0$, K is said to be positively oriented. Otherwise, if $det(K) = 0$ it is said to be degenerated (all the vertices belong to the same hyperplane) [24].

Definition 2. *A set ζ of simplices (triangles in two-dimensional domains, in three-dimensional domains it is*

called tetrahedral) is understood by triangulation of a domain ω which is assumed limited and polyhedral. This set has these conditions:

1. An intersection of two elements of ζ is empty or reduced to one vertex, one edge (in the two-dimensional case) or one face (in the three dimensional case);

2. The union of elements from ζ is equal Ω ;

3. The elements of ζ should be topologically regular: in the two-dimensional case these elements should be as close to the equilateral, which does not require them to be equal [25], [26];

4. Eventually the incidence of the elements will be greater in regions where it is necessary [27].

The Delaunay approach maximizes the smallest angle of all the triangles on the triangulation, thus avoiding much internal sharp angles for optimizing the uniform distribution of itself divisions. This distribution is made by following properties:

- *Maximizing minimum internal angle of the triangles;*
- *Minimizing the maximum circumcircle edges;*
- *Minimizing the maximum minimum edge containment circle.*

III. Methodology

The proposed method was structured in steps, such as indicated in subsection I-B. The organization of the method and the details of each step are detailed in: subsection III-A, with information about strategies to represent the surface landing, mountainous and surfaces shown in [4] and [7]; subsection III-B, with descriptions about the Delaunay triangulation (DT) technique, which was applied to determine candidate positions; subsection III-C, with information about how the candidate positions were selected properly by the sensing radius and the coverage provided by each position; subsection III-D, with details on strategies to minimize the influence of coverage superpositions in the final coverage rate and III-E, with information about the possibility to ensure a connected set and full communication of WSN.

A. Surfaces Representation

The first step was to represent three-dimensional reliefs to test the sensor deployment in the proposed method. This task was performed with the support of the open source graphics package: Blender, which is available under a dual license (BL / GNU General Public License) [28]. The choice of this package allowed to represent different three-dimensional surfaces, from geometric transformations (scale, rotation, rotational translations and others) applied to plans.

The versatility of the proposed method was tested considering surfaces representing different reliefs: the landing relief has 3000 m^2 extension, maximum peak 652 m high and deeper valley with 384 m of depression; the mountainous terrain also has 3000 m^2 extension, but with a maximum peak 1021 m and deeper valley with 403 m of depression. These values were considered in the geometric transformations previously cited. Also, other surfaces were tested to validate the method. The reliefs were selected from available works in literature and which accomplished the criteria: methods developed for deploying sensor nodes, with specifications of the dimensions of the three-dimensional reliefs; coverage radius indication node/sensing; information about the numbers of sensor nodes and area coverage rates. Thus, the methods in [4], [7] present these conditions.

B. Delaunay Triangulation

The second step was the discretization of the surface with the Delaunay triangulation, splitting the geometric domain in simplices. This was possible given the limits as a set of vertices V and s as a k-simplex ($0 \leq k \leq n$), made by the vertices V. A simplex K is a sorted list of the vertex P_i with $1 \leq i \leq d+1$, where d is the dimension of the Euclidean space E. The circumcenter of s was taken as a circumference of radius r touching all vertices of s. If $k = d$, s has a unique circumcenter. The simplex s is Delaunay if there is a circumcenter of s wherein no vertex is inside V. Thus, the edges between the points that satisfy the condition were drawn, generating the Delaunay triangles.

C. Positions Selection

The third step consisted in selecting the candidate positions to solve the MSC problem. The selection was based on the property to obtain communication between candidate positions, indicated by the range of the radius r, which is associated with each position. The radius range is considered omnidirectional.

The selection is made from the positions coverage areas and coverage intersections provided by neighboring candidate positions. The intersection is known when the distance between positions is smaller than twice the radius range r. In the first verifying cycle, the goal is to select candidate positions with the maximum coverage areas without intersections, as illustrated in Fig. 3. In the others cycles, the goal is to establish communication between candidate positions obtained from the first cycle. Communication is understood as coverage intersections between neighboring candidate positions.

Given a pair of selected positions by the first cycle, intermediate positions are searched in the Delaunay triangulation. The intermediate position which provides the highest gain coverage will be selected. The result obtained with this process is illustrated in Fig. 4. As a consequence, a surface area may be covered by sensing one or more candidate positions. This fact produces superpositions which maximizes the WSN coverage area. The algorithm stops when the sum of the coverage area, in the current cycle, less the external and superpositions areas (described in subsection III-D), is less than the value in the previous cycle. The solution of this problem allows to know the real value of coverage with selected positions, ensuring

an acceptable solution to the MSC problem. The solution for superposition is made in the fourth step, subsection III-D

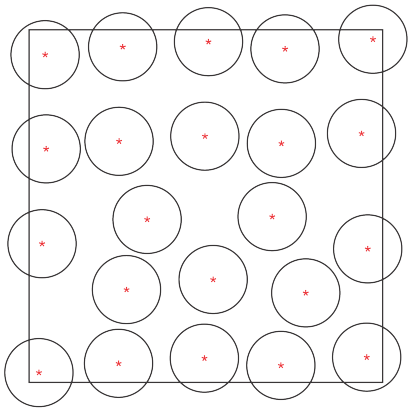

Fig. 3. Illustration of candidate positions without communication, selected with application of the first verifying cycle.

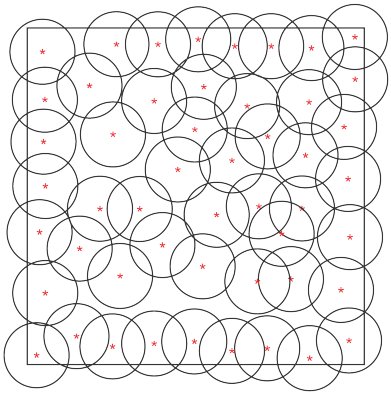

Fig. 4. Illustration of candidate positions with communication obtained from intermediate positions inserts.

D. Solution for superposition

In the fourth step a solution to attend the coverage superposition is proposed, splitting it in two cases: simple superposition and complex superposition. The simple superposition was defined as an area covered by two candidate positions called as i, j. The calculation of the superposition is in Euclidean space R^3 and it was possible using projections of points i', j' in Euclidean space R^2. Also the points defining the intersections between the perimeters of the analyzed areas, which were identified as $n1$ and $n2$, are shown in Fig. 5.

The projection of the positions was possible with the vector

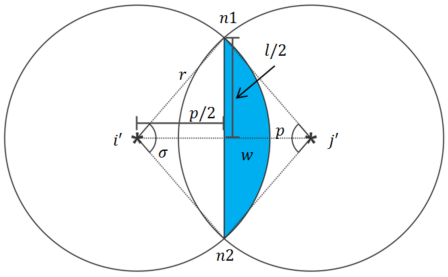

Fig. 5. Simple superposition illustration, as follows: $n1$ and $n2$, intersection points of the circumferences; $i'$and j', selected positions for sensor nodes; p, Euclidean distance between points i' and j'; r, coverage radius showing the communication range of a sensor node; l, Euclidean distance between the points $n1$ and $n2$; σ, angle between the points i', $n1$ and $n2$; w, circular segment area (represented by blue area).

representations, $i' = \begin{bmatrix} 0 \\ 0 \\ 1 \end{bmatrix}$ and $j' = \begin{bmatrix} p \\ 0 \\ 1 \end{bmatrix}$, given that p is the Euclidean distance between i and j in Euclidean space R^3 is given by (1). The definitions of $n1$ and $n2$ occur at the midpoint between i', j', which in this case is defined by $\frac{p}{2}$, and by (2), wherein r is the coverage radius entered by the user and l indicates the Euclidean distance between $n1$ and $n2$. Therefore, the values for $n1$ and $n2$ are given as:

$n1 = \begin{bmatrix} \frac{p}{2} \\ \frac{l}{2} \\ 1 \end{bmatrix}$ and $n2 = \begin{bmatrix} \frac{p}{2} \\ \frac{-l}{2} \\ 1 \end{bmatrix}$.

The parameters described previously are shown in Fig. 5.

$$p = \sqrt{(i_1 - j_1)^2 + (i_2 - j_2)^2 + (i_3 - j_3)^2} \tag{1}$$

$$\frac{l}{2} = \sqrt{r^2 - \left(\frac{p}{2}\right)^2} \tag{2}$$

Let i' be the origin, $n1$, $n2$ and the definition of the angle σ in degrees, with the variation between 0° and 180°, in (4) [29] are necessary to calculate the area superposition w, which is given in (3) [30]. The area superposition w for removal is shown in Fig. 5:

$$w = \frac{r^2}{2}\left(\frac{\pi}{180} - \sin\sigma\right), \tag{3}$$

where r is the coverage radius (given by the user) and is associated with each candidate position.

$$\sigma = acos\,(\vartheta)\,\frac{180}{\pi}, \tag{4}$$

where ϑ is the angle in radians made by $n1$ and $n2$ is given by (5):

$$\vartheta = \frac{n2^t n1}{\|n1\|\,\|n2\|}. \tag{5}$$

The complex superposition was defined by an area covered by more than two candidate positions. To solve this situation it was necessary to calculate the central areas given by T, and adjacency neighboring. The number of adjacent areas depends

on the number of candidate positions involved. For given a covered area by three candidate positions (i, j, k), there are three adjacent areas (A, B, C) and the central area (T) as seen in Fig.7. The definitions of the areas were defined by projections of candidate positions. Considering the example of superposition generated by three candidate positions, the distances ik, edge a, kj, edge b, and ji, edge p, the angles α, β and γ were calculated applying the strategy described in simple superposition. These parameters were calculated in (1) and (6), and their spacial representation are shown in Fig. 6. The results are projected regions as shown in Fig. 8.

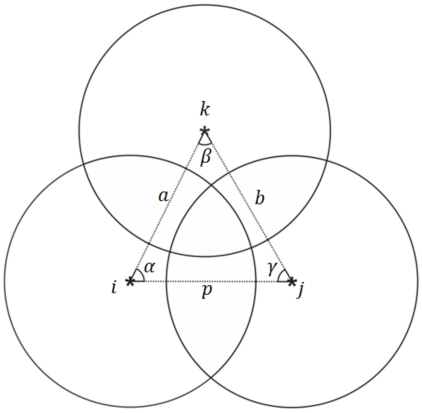

Fig. 6. Superposition representation of coverage areas with three neighboring positions in Euclidean space R^3, where: i, j and k are selected positions for sensor nodes; a,b ,c , are Euclidean distances among points ik, kj and ji, α, β and γ are angles generates by the points jik, ikj and kji, respectively

$$k' = M \times i', \tag{6}$$

where $M = \begin{bmatrix} 1 & & a \times \cos\alpha \\ & 1 & a \times \sin\alpha \\ & & 1 \end{bmatrix}$ and $i' = \begin{bmatrix} 0 \\ 0 \\ 1 \end{bmatrix}$

are given in homogeneous coordinates, i' and k' are projections in Euclidean space R^2, a shows the Euclidean distance between points i and k, α is the angle generate by the edges ik and ij.

The projection j' was given by $j' = \begin{bmatrix} p \\ 0 \\ 1 \end{bmatrix}$, in homogeneous coordinates, which p is the Euclidean distance between i and j as shown in (1). After projecting j' and k' it is verified if the sum of the angles α, β, γ is equal to 180°, to check the formation of a triangle such as shown in Fig. 6.

The central area T is obtained by calculating the Euclidean distances of the intersection points of the perimeters from a pair of candidate positions called P, a candidate position was given as the reference and belongs to P. The intersection point of the perimeter with the minimum distance of the candidate position in P is chosen to determine the center area defined as T. Thus, considering the pairs of positions $i'k'$, $k'j'$ and $j'i'$, with the corresponding points $y1$ to $y6$, the calculated

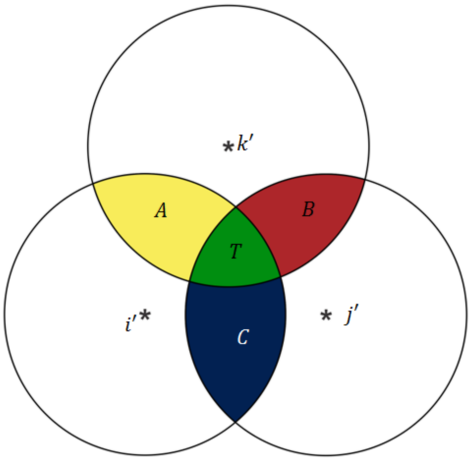

Fig. 7. Superposition representation with triple intersected areas, as follows: i', j' and $k'$are selected positions; A, B, C, are removed areas of simple superposition and T is the double superposition area (represented by the green area).

Euclidean distances are obtained for the edges: $y1$ and j', $y2$ and j', $y3$ and i', $y4$ and i', $y5$ and k', $y6$ and k'.

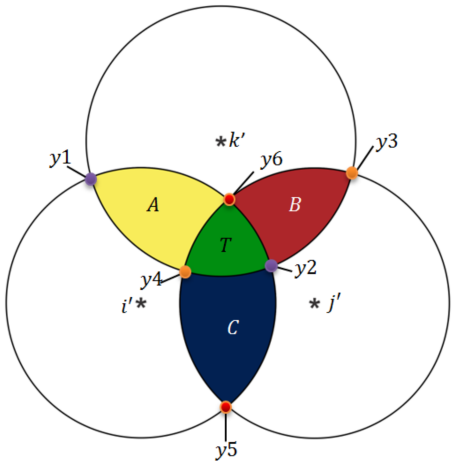

Fig. 8. Superposition representation of three coverage areas, as follows: $y1$, $y2$, $y3$, $y4$, $y5$ and $y6$ are intersection points among the circumferences; i' , j' and k' are selected positions for sensor nodes; A, B, C, are the removed areas of the simple superposition and$T$ is the double superposition area (represented by green area).

Afterwards the identification of the intersection points $y2$, $y4$ and $y6$, which are the vertices of the central region T, shown in Fig. 9, the area value is calculated splitting T in sub-regions: the triangle, defined by Ta and segments of circle, represented by m, n and o, is illustrated in Fig. 9.

The triangle area Ta was calculated by the Heron's formula [31], from the edges e, f and g of the triangle obtained previously. Thus, Ta is given by (7):

$$Ta = \sqrt{pm(pm-e)(pm-f)(pm-g)}, \tag{7}$$

which pm is the semiperimeter of the triangle set composed by the edges e, f and g, in (8).

$$pm = \frac{e + f + g}{2}. \tag{8}$$

The removal of the external areas used techniques shown in the subsections III-D using as reference the edges of the area of interest for the areas removal, as illustrated in Fig. 10.

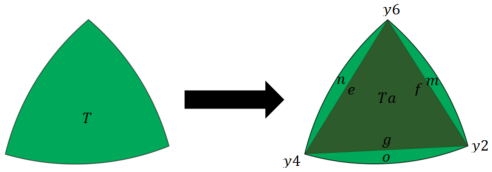

Fig. 9. Splitting of the central region T in sub-regions: the triangle Ta consists on the edges e, f and g; and the segments of circle m, n and o are areas defined by the vertices $y2$, $y4$ and $y6$.

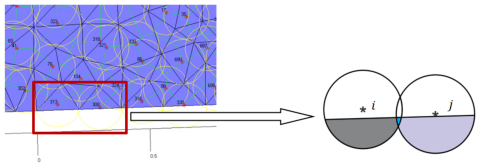

Fig. 10. Problem of external coverage (left) and the selected sensor nodes for removal the external area (right).

E. Communication check

The communication among the positions was verified by using the Prim's algorithm for minimum spanning trees [32]. The algorithm was chosen due to its minimal spanning tree generation feature using a unique set. Combining this algorithm with the given radius, it was possible to check if all selected positions are contained in a unique set. This property guarantees the communication among the candidate positions.

IV. Results and Discussion

The versatility of the method is shown with deployment sensor nodes in distinct reliefs, as detailed in subsection III-A. The simulations were performed with a sensing radius of 100 meters. The proposed method was performed to the landing surface and obtained the coverage area of 84,92%, with 323 selected positions. The candidate positions for sensors nodes are shown in Fig. 11, represented by red asterisks. For the mountainous terrain, the method obtained the maximum coverage rate (85,62% of coverage area) with 434 selected positions. The selected positions indicated by red asterisks are illustrated in Fig 12.

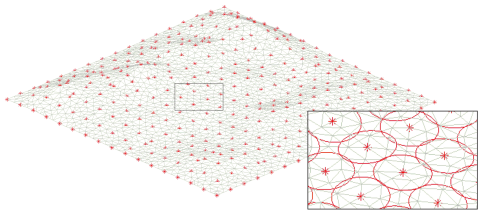

Fig. 11. Visualization of candidate positions for the landing surface.

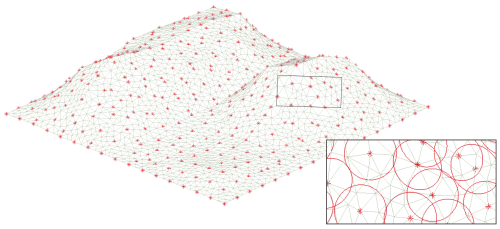

Fig. 12. Visualization of candidate positions for the mountainous surface.

A. Comparisons

The performances of the proposed method were compared to the methods developed by [4], [7], according to conditions presented in subsection III-A. The surfaces described by the authors have about 1000 m^2 of area, with approximations illustrated in Fig. 13.

The proposed method developed by [4] considered a sensing radius of 25 meters and deployed 2800 sensor nodes to obtain 46% of coverage area. The sensing rate by each sensor node is about 0,0164%. Considering the surface used by the author with the same radius, the deploying of our method is shown in Fig. 14, with 831 selected positions and coverage rate of 95,29%. The coverage rates by each sensor node (0,1147%) are greater than those provided by [4]. Generating a greater coverage and a reduction in the number of sensor nodes used in about 70%.

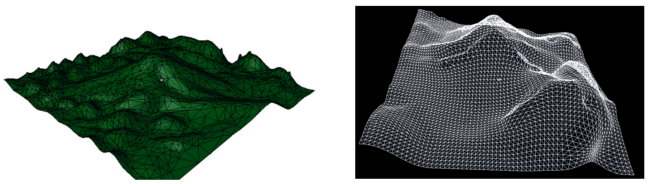

(a) approximation given by [4] (b) approximation given by [7]

Fig. 13. Surface's representations for comparisons.

The technique developed by [7] simulated distributions with a communication radius of 60 meters. The best result was a

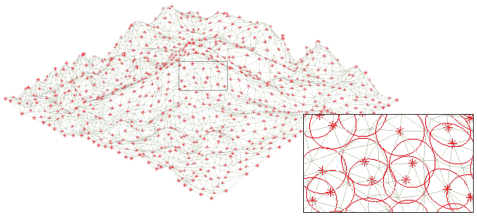

Fig. 14. Visualization of candidate positions (red asterisks) for the surface explored by [4].

coverage rate of about 98%, with 400 sensor nodes deployed. These values provide a rate of 0,2450% of coverage by each sensor node. The result of the deployment obtained with our method, considering the surface given by [7] and the same sensing radius is shown in Fig. 15. The coverage rate with our proposal was 91,10% of coverage area, deploying 160 sensor nodes. Although the coverage is smaller then the result provided by [7], the proposed method needed only 40% of the total number of positions used by [7] to obtain a relevant result: only 6,9% of difference. Furthermore, the coverage area by sensor node was 0,5694%, showing our method provides better coverage per unit.

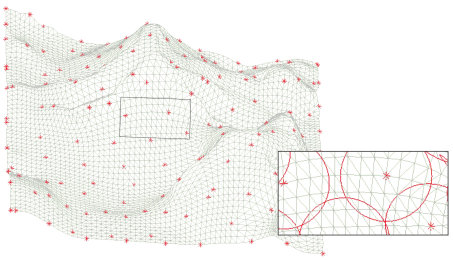

Fig. 15. Visualization of candidate positions (red asterisks) for relief represented by [7].

V. Conclusion

The deployment problem by using a minimum number of devices is considered NP-Hard type [10]. For this problem, the solutions were developed and measured by applying heuristic approach. Even then, from the researched works, it can not be assured which is the unique solution to obtain the same quality of coverage for all explored surfaces [12], [33]. An appropriate deployment could ensure a WSN with fewer communication failure, lower energy consumption and positioning errors of the sensor nodes.

The method proposed in this paper considered the Delaunay triangulation as a different strategy to initial distributions given by the works available in literature, such as [4], [7]. An important advantage of the method was to define the deployment in distinct types of three-dimensional surfaces, as shown in our results. Also, similar studies were not found considering the problem of coverage superposition as we performed in this work. The strategies adopted were important to allow a realistic treatment of the problem of minimum set coverage and the ensure of the method is useful for practical design of a WSN.

In comparative tests, the method showed interesting results and was more efficient for deployment of sensor nodes. This statement is possible when we observe the coverage rate by position: our results exceeded those provided by [4] and [7]. In comparisons with those works, our proposal provides greater coverage per unit. Also, coverage rates above 90% in realistic and complex surfaces indicates that the method is promising and could contribute to the development of WSN area. As suggestions for future work, a complement is to obtain deployment by the Voronoi diagram, considering the duality of the Delaunay triangulation.

Acknowledgment

This work is supported by the CNPq under the process 133023/2015-0.

References

[1] H. Karl and A. Willig, *Protocols and architectures for wireless sensor networks*. John Wiley & Sons, 2007.

[2] A. Ghosh and S. K. Das, "Coverage and connectivity issues in wireless sensor networks: A survey," *Pervasive and Mobile Computing*, vol. 4, no. 3, pp. 303–334, 2008.

[3] C.-H. Wu, K.-C. Lee, and Y.-C. Chung, "A delaunay triangulation based method for wireless sensor network deployment," *Computer Communications*, vol. 30, no. 14, pp. 2744–2752, 2007.

[4] S. Oktug, A. Khalilov, and H. Tezcan, "3d coverage analysis under heterogeneous deployment strategies in wireless sensor networks," in *Telecommunications, 2008. AICT'08. Fourth Advanced International Conference on*. IEEE, 2008, pp. 199–204.

[5] C.-Y. Chang, C.-T. Chang, Y.-C. Chen, and H.-R. Chang, "Obstacle-resistant deployment algorithms for wireless sensor networks," *Vehicular Technology, IEEE Transactions on*, vol. 58, no. 6, pp. 2925–2941, 2009.

[6] M. R. Ingle and N. Bawane, "An energy efficient deployment of nodes in wireless sensor network using voronoi diagram," in *Electronics Computer Technology (ICECT), 2011 3rd International Conference on*, vol. 6. IEEE, 2011, pp. 307–311.

[7] D. Li and H. Liu, "Sensor coverage in wireless sensor networks," *Wireless Networks: Research, Technology and Applications'(Nova Science Publishers, 2009)*, pp. 3–31, 2009.

[8] M. Jin, G. Rong, H. Wu, L. Shuai, and X. Guo, "Optimal surface deployment problem in wireless sensor networks," in *INFOCOM, 2012 Proceedings IEEE*. IEEE, 2012, pp. 2345–2353.

[9] N. Unaldi, S. Temel, and V. K. Asari, "Method for optimal sensor deployment on 3d terrains utilizing a steady state genetic algorithm with a guided walk mutation operator based on the wavelet transform," *Sensors*, vol. 12, no. 4, pp. 5116–5133, 2012.

[10] J.-Y. Lee, J.-H. Seok, and J.-J. Lee, "Multiobjective optimization approach for sensor arrangement in a complex indoor environment," *Systems, Man, and Cybernetics, Part C: Applications and Reviews, IEEE Transactions on*, vol. 42, no. 2, pp. 174–186, 2012.

[11] J.-H. Seok, J.-Y. Lee, W. Kim, and J.-J. Lee, "A bipopulation-based evolutionary algorithm for solving full area coverage problems," *Sensors Journal, IEEE*, vol. 13, no. 12, pp. 4796–4807, 2013.

[12] Y. Yoon and Y.-H. Kim, "An efficient genetic algorithm for maximum coverage deployment in wireless sensor networks," *Cybernetics, IEEE Transactions on*, vol. 43, no. 5, pp. 1473–1483, 2013.

[13] F. M. Al-Turjman, H. S. Hassanein, and M. Ibnkahla, "Quantifying connectivity in wireless sensor networks with grid-based deployments," *Journal of Network and Computer Applications*, vol. 36, no. 1, pp. 368–377, 2013.

[14] M. Vecchio and R. López-Valcarce, "Improving area coverage of wireless sensor networks via controllable mobile nodes: A greedy approach," *Journal of Network and Computer Applications*, vol. 48, pp. 1–13, 2015.

[15] K. Arthi, A. Vijayalakshmi, and P. V. Ranjan, "Critical event based multichannel process control monitoring using wsn for industrial applications," *Procedia Engineering*, vol. 64, pp. 142–148, 2013.

[16] C.-Y. Chong and S. P. Kumar, "Sensor networks: evolution, opportunities, and challenges," *Proceedings of the IEEE*, vol. 91, no. 8, pp. 1247–1256, 2003.

[17] C. Hartung, R. Han, C. Seielstad, and S. Holbrook, "Firewxnet: A multitiered portable wireless system for monitoring weather conditions in wildland fire environments," in *Proceedings of the 4th international conference on Mobile systems, applications and services*. ACM, 2006, pp. 28–41.

[18] A. Mainwaring, D. Culler, J. Polastre, R. Szewczyk, and J. Anderson, "Wireless sensor networks for habitat monitoring," in *Proceedings of the 1st ACM international workshop on Wireless sensor networks and applications*. ACM, 2002, pp. 88–97.

[19] K. Delin, R. Harvey, N. Chabot, S. Jackson, M. Adams, D. Johnson, and J. Britton, "Sensor web in antarctica: Developing an intelligent, autonomous platform for locating biological flourishes in cryogenic environments," in *Lunar and Planetary Science Conference*, vol. 34, 2003, p. 1929.

[20] Q. A. Al-Haija, H. Al-Qadeeb, and A. Al-Lwaimi, "Case study: Monitoring of air quality in king faisal university using a microcontroller and wsn," *Procedia Computer Science*, vol. 21, pp. 517–521, 2013.

[21] S.-C. Bae, W.-S. Jang, S. Woo *et al.*, "Prediction of wsn placement for bridge health monitoring based on material characteristics," *Automation in Construction*, vol. 35, pp. 18–27, 2013.

[22] B. Delaunay, "Sur la sphere vide," *Izv. Akad. Nauk SSSR, Otdelenie Matematicheskii i Estestvennyka Nauk*, vol. 7, no. 793-800, pp. 1–2, 1934.

[23] D.-Z. Du and F. Hwang, *Computing in Euclidean geometry*. World Scientific, 1995, vol. 4.

[24] P. George and F. Hermeline, "Delaunay's mesh of a convex polyhedron in dimension d. application to arbitrary polyhedra," *International Journal for Numerical Methods in Engineering*, vol. 33, no. 5, pp. 975–995, 1992.

[25] I. Babuška and A. K. Aziz, "On the angle condition in the finite element method," *SIAM Journal on Numerical Analysis*, vol. 13, no. 2, pp. 214–226, 1976.

[26] P. G. Ciarlet, *The finite element method for elliptic problems*. Siam, 2002, vol. 40.

[27] W. Thacker, "A brief review of techniques for generating irregular computational grids," *International Journal for Numerical Methods in Engineering*, vol. 15, no. 9, pp. 1335–1341, 1980.

[28] T. Roosendaal, *BLENDER LICENCE 1.0*. https://www.blender.org/BL/, 2005.

[29] R. M. Milne, *Mensuration and Elementary Solid Geometry for Schools*. The University Press, 1923.

[30] B. Hahn and D. Valentine, *Essential MATLAB for engineers and scientists*. Newnes, 2007.

[31] A. S. Posamentier and I. Lehmann, *The secrets of triangles: a mathematical journey*. Prometheus Books, 2012.

[32] R. C. Prim, "Shortest connection networks and some generalizations," *Bell system technical journal*, vol. 36, no. 6, pp. 1389–1401, 1957.

[33] M. R. Garey and D. S. Johnson, "A guide to the theory of np-completeness," *WH Freemann, New York*, 1979.